Cavity Filtered Injection Locking for Large Angle Atomic Interferometry

by

Thomas John Liptay

Submitted to the Department of Electrical Engineering and Computer Science
and
Department of Physics
in partial fulfillment of the requirements for the degrees of
MEng in Electrical Engineering and Computer Science
and
Bachelor of Science in Physics
at the
MASSACHUSETTS INSTITUTE OF TECHNOLOGY
August 2000

Author .....
Department of Electrical Engineering and Computer Science
and
Department of Physics
August 18, 2000

Certified by 8/18/00
Selim Shahriar
Research Scientist
Thesis Supervisor

Accepted by .....
David E. Pritchard
Senior Thesis Coordinator
Department of Physics

Accepted by .....
Arthur C. Smith
Chairman, Department Committee on Graduate Students
Department of Electrical Engineering and Computer Science

Cavity Filtered Injection Locking for Large Angle Atomic Interferometry

by

Thomas John Liptay

Submitted to the Department of Electrical Engineering and Computer Science
and
Department of Physics
on August 18, 2000, in partial fulfillment of the
requirements for the degrees of
MEng in Electrical Engineering and Computer Science
and
Bachelor of Science in Physics

Abstract

Many experiments in atomic physics require two laser beams with a controllable difference in frequencies. In this thesis, I report on realizing this goal using a technique where an electro-optic modulator sideband is filtered through a cavity and injected into a diode laser, in a novel configuration yielding very high feedback isolation without sacrificing access to the output power of the diode laser. The advantages of this approach over alternative techniques for injection locking are discussed. I explain how this injection locking technique is being used in the construction of a large angle atomic interferometer based on a novel Raman pulse beam splitting technique. After theoretically deriving a Raman transition from basics quantum mechanics, an explanation of Raman pulse beam splitting is given. Our experimental setup and experimental results are discussed. Finally, experiments that we have performed, including magnetic sublevel optical pumping and a Ramsey fringe experiment, along with their results are presented.

Thesis Supervisor: Selim Shahriar
Title: Research Scientist

Acknowledgments

First, I would like to thank Selim Shahriar for supervising my thesis and giving me the chance to work on an extremely interesting experiment. Selim is an excellent teacher and is responsible for teaching me all of the theory behind the experiment.

I would also like to thank Ying for being such a fun and nice partner to work with. You made daily life the lab an enjoyable experience and tolerated my constant stream of questions and pessimism. Thanks Alex for being a fun partner to work with. You taught me a lot and made life in the lab good and easy. You're jokes were greatly appreciated. Thanks also to Jacob, John, Jack, Joe, Aaron, Parminder, and the rest of the people in the lab who made my time memorable.

I would especially like to thank my parents for supporting me in all that I choose to do. Thanks for paying for my education at MIT and providing me with a home that I could always return to to relax. You are wonderful parents. I will always love you.

Contents

1 Introduction **8**

2 Large Angle Atomic Interferometer **10**

2.1 Basic Idea 10

2.2 Interaction of Atoms with Light 12

2.2.1 Two Level Atom 12

2.2.2 Raman Transition 14

2.3 Raman Pulse Beam Splitting 20

2.3.1 One Dimensional 20

2.3.2 Two dimensional 22

3 Injection Locking a Diode Laser Using a Filtered Electro-Optic Modulator Sideband **24**

4 Experimental Results **31**

4.1 Basics of the Atomic Beam 31

4.2 Single Zone Co-Propagating Raman 32

4.3 Magnetic Sub-level Optical Pumping 34

4.4 Ramsey Fringes 35

5 Conclusion **38**

A Figures **39**

List of Figures

A-1 Shows the basic idea behind the interference experiment. The splitting and recombining of the atomic beam, represented here by dashed lines, is achieved using a series of Raman pulses. The diagram shows that the depostion of atoms on the plate forms an interference pattern. . . 40

A-2 Two laser beams with frequencies, ω_1 and ω_2 are applied to a three level atom to cause a Raman transition. δ is the common detuning of the laser beams. Δ is the relative detuning of the laser beams 41

A-3 Shows the relevent energy levels of ^{85}Rb. 42

A-4 Shows the first three Raman pulses used to split the atomic beam and the state of the atoms after each pulse. The first pulse, A0 and C0, is a $\frac{\pi}{2}$ pulse and puts the atoms in an equal superposition of $|a\rangle$ and $|c\rangle$. The next two π pulses give the two components of the atomic momentum in opposite directions. 43

A-5 Shows two dimensional Raman pulse beamsplitting applied to atoms falling from a magnetic trap. First the atoms are split along the z axis. Immediately after Raman pulses are applied to recombine the atoms in the z direction, the atoms are split along the x axis. After applying another set of Raman pulses to recombine the atoms in the x direction, all four components of the atomic beam come together to form a two dimensional interference pattern. The dimensions of the interference pattern are determined by the number of Raman pulses used to split and recombine the atoms. 44

A-6 Shows a schematic of the setup used to lock a diode laser to the sideband of a cavity filtered EOM shifted beam. A modified isolator is used to convert cross polarized beams to beams with the same polarization. The Fabry Perot cavity only allows the portion of the Ti-Sapphire beam that is upshifted by the EOM to pass through it. The combination of the polarizing beam splitter, neutral density filter, and $\frac{\lambda}{4}$ plate are used to minimize the diode laser power that is reflected off of the cavity and back to the diode laser. 45

A-7 a) Shows a how a normal isolator works. The combination of two polarizers with a Faraday rotator between them ensures that power can only pass through the isolator in one direction. b) Shows how we modified an isolator by removing the polarizer oriented at 45 degrees. The result is that beams that are corss polarized on the right hand side can be polarized in the same direction on the left hand side. 46

A-8 Shows a beatnote generated by mixing the injection locked diode laser with a beam from the Ti-Sapphire laser. 47

A-9 The transit-time limited Raman-Ramsey fringes obtained for the magnetic field insensitive component of the off-resonant Raman transition in ^{85}Rb atomic beam. 48

A-10 Schematic of Experimental Setup. A solid sample of Rb is heated in an oven to form Rb vapor. Some Rb atoms escape from the oven through a hole and are collimated by an aperture to form the atomic beam. Optical pumping and Raman beams can be appied to the atoms as they travel the length of the atomic beam. A detection beam excites atoms in $|3\rangle$. A photo multiplier tube is used to detect photons emitted by excited atoms during spontaneous emission. 49

A-11 Plots fluorescence detected by the PMT when one Raman beam is applied as a function of the EOM frequency shift. The peak occurs when the relative detuning of the two Raman beams is zero. (Note: fluorescence is highest at the bottom of the graph and lowest at the top of the graph.) 50

A-12 Shows fluorescence plotted versus EOM frequency shift for a set of co-propagating Raman beams when a magnetic field is applied. The magnetic field splits the energies of the magnetic sublevels of $|F = 2\rangle$. The populations of the 5 magnetic sublevels of $|2\rangle$ are about equal. . 51

A-13 Shows the effects of magnetic sublevel optical pumping. The majority of the atoms have been moved to the $m_f = 0$ state. 52

A-14 Shows the two Raman pulses used to see Ramsey fringes and their Fourier transform. The top of the diagram shows the two Raman pulses separated by time τ rewritten in terms of a convolution of two delta functions with a single pulse. The bottom shows how the Fourier transform of the two pulses can be found by multiplying the Fourier transform of the two delta functions with the Fourier transform of a single pulse. 53

Chapter 1

Introduction

There is currently a lot of interest in being able to create structures on the nanometer scale. Micro-electromechanical devices (MEMs) have proven to be very useful and promise to become even more important in the future. Also, integrated cricuits have been getting progressively smaller and there is concern that a new fabrication technique will need to be developed if circuits continue to shrink at the rate that they have been for the last few decades. One thing is for certain though: the current trend is to create smaller and smaller devices. The ultimate goal is to be able to control the placement of individual atoms in order to make the smallest possible devices.

In Dr. Shahriar's lab, work is progressing on an experiment which is the first step to being able to create nanometer scale structures. We plan to use a novel Raman pulse beamsplitting technique in order to split and recombine an atomic to create nanometer structures. For example, there is currently a proposal to use a regular array of quantum dots to create a quantum computer, but fabricating such an array is not currently possible. However, if our experiment is successful, then the interferometer could be used to create a two dimensional array of regularly spaced quantum dots with spacings of only a few nanometers. Also, ultra precise diffraction gratings could be produced with a one dimensional version of the interferometer. A more immediate use for the interferometer is to detect extremely small rotations. If the beam splitting technique works in an atomic beam, then the same ideas could be applied to atoms falling from a magneto-optic trap to create a device capable of measuring rotations of

10^{-14} radians/second, more sensitive than anything existing today. This sensitivity is enough to be able to measure the Lens-Thirring rotation due to the rotation of the sun. This prediction of general relativity has never been observed because of a lack of sensitive enough measuring devices. Ultimately, the beam splitting and recombining technique used in the large angle atomic interferometer could be modified so that people are able to control the placement of individual atoms and hence create arbitrary structures on the atomic level.

Chapter 2 discusses the theory behind how we plan to split and recombine the atomic beam. First, the quantum mechanics behind a Raman transition is discussed since this is the basis for all of the beam splitting. Then an explanation of how an atomic beam can be split and recombined using the proper sequence of Raman pulses is given. After explaining the theory behind a one dimensional beamsplitter, I explain how a two dimensional beamsplitter can be constructed using the same beam splitting technique.

The Raman pulse beam splitting technique requires two sufficiently powerful laser beams with a controllable frequency difference in order to split the atomic beam. Chapter 3 explains how we achieved this by modelocking a diode laser to a cavity filtered EOM sideband. Details of our experimental setup are discussed, including how a modified isolator was used in conjunction with a polarizing beamsplitter to prevent the diode laser beam from feeding back to itself. Experimental data that was obtained using this technique is presented.

Chapter 4 discusses preliminary experiments that have been performed along with their results. The theory and experimental results for both magnetic sublevel optical pumping and a Ramsey fringe experiment are presented.

Cahpter 5 summarizes how far the large angle atomic interferometer has progressed and discusses what still needs to be done to create a working interferometer.

Chapter 2

Large Angle Atomic Interferometer

This chapter explains the theory behind the large angle atomic interferometer. First the basic idea behind any atomic interferometer is discussed. Then the details of the quantum mechanics behind our experiment are discussed. As mentioned before, our plan is to use a series of Raman pulses in order to split and recombine the atomic beam. In section 2 the quantum mechanics of atoms interacting with light is discussed. First the theory of two level atoms interacting with an electromagnetic field is reviewed. Then a Raman transition in a three level atom is derived. Section 3 explains how we plan to use a series of pulsed Raman transitions to split and recombine the atomic beam. After explaining a simple one dimensional version of the interferometer, the ideas are extended to show how to create a two dimensional interference pattern.

2.1 Basic Idea

In the early twentieth century people discovered that anything that could carry momentum, light or matter, has a wave nature as well as a particle nature. Wavelength is related to momentum via Planck's constant, $p = \frac{h}{\lambda}$. There are many familiar examples of interference occurring with light. Both Michelson Morley interferometers and double slit experiments demonstrate that light has a wave length and can be made to interfere with itself. In our experiment we plan to use the wave nature of atoms

to generate an interference pattern.

In a typical interference experiment involving light, a monochromatic light beam is split into two parts. The two parts of the light beam are then reflected off of mirrors so that they come together at an angle on a viewing surface. (See figure A-1). At a particular point on the viewing surface the direction of the electromagnetic field due to one of the light beams may cancel the field due to the other beam. In this case there will be destructive interference and no photons will be detected at that particular point on the viewing surface. Likewise, at other points the fields of the two light beams will add constructively to give a strong flux of photons. If the two incoming beams can be approximated as plane waves – as they usually can – then a sinusoidal interference signal will result. The greater the angle between the two incoming beams, the finer the interference fringes will be. Also, if the phase of one of the incoming beams is shifted – for example by changing the path length of one of the beams – then the positions of the interference fringes will shift accordingly.

Our interference experiment is exactly the same as interference experiments involving light, only we use atoms. The basic idea is that if we can spatially split an atomic beam into two parts and recombine the two parts of the split atomic beam, then we will be able see interference between the atoms on a plate. Researchers have already performed atomic interference experiments and seen the predicted results. The large angle atomic interferometer experiment is new because of the novel method of splitting and recombining the atomic beam. If successful, the atomic beam will be split far more that has been achieved previously, and hence will be able to produce finer interference fringes.

If a wave is split into two parts and recombined, then one dimensional interference fringes will result. However, if the beam is split into four parts in two dimensions and recombined, then a two dimensional interference pattern will result. This is exactly what we plan to do with our atomic beam. The following section explains the quantum mechanics behind Raman transitions, which is the basis of our beam splitting and recombining technique.

2.2 Interaction of Atoms with Light

This section presents a theoretical derivation of a Raman transition starting from basic perturbation theory. First, Rabi flopping of a 2 level atom interacting with an electromagnetic field is explained. Then, a Raman transition in a 3 level atom interacting with two lasers is derived.

2.2.1 Two Level Atom

Consider a 2 level atom in free space with a ground state $|g\rangle$ and an excited state $|e\rangle$. Neglecting interactions with the environment that cause spontaneous emission, the Hamiltonian H_o for the atom in the $\{|g\rangle, |e\rangle\}$ basis is

$$H_o = \begin{bmatrix} E_g & 0 \\ 0 & E_e \end{bmatrix} \tag{2.1}$$

where E_g is the energy of the atom in its ground state and E_e is the atom's energy when it is in its ground state. The most general solution to the Shrödinger equation, $i\hbar\frac{\partial}{\partial t}|\psi\rangle = H|\psi\rangle$, with this Hamiltonian is $|\psi\rangle = C_g(0)e^{-i\omega_g t}|g\rangle + C_e(0)e^{-i\omega_e t}|e\rangle$ where $\omega_{g,e} = \frac{E_{g,e}}{\hbar}$. Because we neglected spontaneous emission, an atom initially in the excited state $|e\rangle$ will remain in the excited state indefinently.

If an electromagnetic field is applied to the atom, then a perturbation V must be added to the unperturbed Hamiltonian H_o. According to classical physics the energy of a dipole $\overrightarrow{p}$ in an electric field is given by $V = -\overrightarrow{p} \cdot \overrightarrow{E}$. We will model the interaction between an atom and an electromagnetic field using this expression for V where $\overrightarrow{p} = e\overrightarrow{r}$ is the dipole moment of the atom and $\overrightarrow{r}$ is the position operator of the valence electron in the atom. Assuming an electric field of the form $\overrightarrow{E} = \overrightarrow{E_o}\cos\nu t$, the perturbation V can be written in matrix form as

$$V = \begin{bmatrix} 0 & \wp E_o \cos\nu t \\ \wp^* E_o^* \cos\nu t & 0 \end{bmatrix} \tag{2.2}$$

where $\wp$ is the component of the atom's dipole moment $\langle e|e\overrightarrow{r}|g\rangle$ in the direction of

$\vec{E}$. Both $\langle e|V|e\rangle$ and $\langle g|V|g\rangle$ are zero because the expectation value for the position of an electron in an atom in either $|e\rangle$ or $|g\rangle$ is zero, ie $\langle e|\vec{r}|e\rangle = \langle g|\vec{r}|g\rangle = 0$. This is true due to symmetry.

In order to simplify the mathematics we can view the system from a rotating frame. To do this we rewrite the wavefunction for the atom as

$$|\psi\rangle = C_g(t)e^{i(-\frac{1}{2}\delta-\omega_g)t}|g\rangle + C_e(t)e^{i(\frac{1}{2}\delta-\omega_e)t}|e\rangle \tag{2.3}$$

where $\delta = \omega - \nu$ and $\omega = \omega_e - \omega_g$. (Note: In this picture C_g and C_e differ from the previously defined coefficients by a phase factor.) After substituting $|\psi\rangle$ into the Shrödinger equation with the total Hamiltonian $H = H_o + V$ and multiplying both sides by $\langle e|e^{-i(-\frac{1}{2}\delta-\omega_e)t}$ we find - after some algebra – that

$$i\hbar\frac{\partial}{\partial t}C_e - \frac{1}{2}\delta\hbar C_e = -\wp E_o C_g e^{i\nu t}\cos\nu t \tag{2.4}$$

By breaking the cos into complex exponentials we can rewrite the right hand side as $\wp E_o C_g e^{i\nu t}\cos\nu t = \frac{1}{2}\wp E_o C_g + \frac{1}{2}\wp E_o C_g e^{2i\nu t}$. Because $e^{2i\nu t}$ oscillates at optical frequencies and C_e and C_g change at a much slower rate, we can neglect the $\wp E_o e^{2i\nu t}$ term, since its average value is zero, and approximate $\wp E_o C_g e^{i\nu t}\cos\nu t$ as $\frac{1}{2}\wp E_o C_g$. This is a common approximation called the rotating wave approximation. Basically, we have rewritten the $\cos\nu t$ in the $\langle g|V|e\rangle$ matrix element as $\frac{1}{2}e^{-i\nu t}$, since we determined that the $\frac{1}{2}e^{i\nu t}$ part of the cos could be neglected. A similar argument can be made for the $\langle e|v|g\rangle$ matirx element. After the rotating wave approximation the total Hamiltonian $H = H_o + V$ becomes

$$H = \begin{bmatrix} E_e & -\frac{\Omega}{2}e^{-i\nu t} \\ -\frac{\Omega^*}{2}e^{i\nu t} & E_g \end{bmatrix} \tag{2.5}$$

where $\Omega \equiv \wp E_o$. In order to simplify the mathematics, it is convenient to deal with a time independent Hamiltonian. By performing a unitary transformation the Hamiltonian H can be transformed to a time independent form. Let Q be a unitary matrix, ie $QQ^\dagger = I$, that has the property that $\dot{Q} = MQ$ where M is time independent.

Multiplying both sides of the Shrödinger equation by Q and defining $|\Psi\rangle \equiv Q|\psi\rangle$, we find – remembering that $|\dot{\Psi}\rangle = \dot{Q}|\psi > +Q|\dot{\psi}\rangle$ – that $i\hbar|\dot{\Psi}\rangle = (\tilde{H} + i\hbar M)|\Psi\rangle$ where $\tilde{H} \equiv QHQ^{\dagger}$. The goal is to choose Q so that $\tilde{\tilde{H}} \equiv \tilde{H} + i\hbar M$ is time independent. Letting

$$Q = \begin{bmatrix} e^{i\theta_1 t} & 0 \\ 0 & e^{i\theta_2 t} \end{bmatrix} \tag{2.6}$$

yields

$$M = \begin{bmatrix} i\theta_1 & 0 \\ 0 & i\theta_2 \end{bmatrix} \tag{2.7}$$

This choice of Q clearly satisfies the above conditions: $QQ^{\dagger} = I$ and $\dot{Q} = MQ$ where M is independent of time. By choosing $\theta_1 = \frac{1}{2\hbar}(E_e + E_g + \hbar\nu)$ and $\theta_2 = \frac{1}{2\hbar}(E_e + E_g - \hbar\nu)$ we find that

$$\tilde{\tilde{H}} = \frac{1}{2}\begin{bmatrix} -\delta & \Omega \\ \Omega^* & \delta \end{bmatrix} \tag{2.8}$$

This Hamiltonian governs the evolution of a 2 level atom interacting with light. If the light is resonant with the atom, $\delta = 0$, then it is easy to see that the solutions to the Shrödinger equation are sinusoids, ie if an atom is intially in the ground state then the probability of finding that atom in the excited state is $|\sin\frac{\Omega T}{2}|$. Thus, an atom initially in state $|g\rangle$ will evolve into an atom in state $|e\rangle$ in a time $T = \frac{\pi}{\Omega}$ and vice versa. A pulse of radiation that lasts for a time T is called a π pulse. If the detuning is nonzero, $\delta \neq 0$, then the probability of finding an atom, initially in the ground state, in the excited state varies sinusoidally in time, but the atom never becomes fully excited. All of this is clear if one solves the Shrödinger equation with $\tilde{\tilde{H}}$.

2.2.2 Raman Transition

Three energy levels of an atom are involved in a Raman transition. For this section a 3 level atom will be considered where $|1\rangle$ and $|2\rangle$ are ground states of the atom with

different energies and $|3\rangle$ is an excited state. For the following derivation we will let ΔE_1 and ΔE_2 denote the energy differences between the ground states, $|1\rangle$ and $|2\rangle$, and the excited state $|3\rangle$ respectively.

Suppose that we shine two laser beams with different frequencies, ω_1 and ω_2, at a 3 level atom. Following an analysis similar to that for the two level atom, the Hamiltonian for a 3 level atom interacting with the two electromagnetic fields can be written in the $\{|1\rangle, |3\rangle, |2\rangle\}$ basis as

$$\mathbf{H} = \begin{bmatrix} E_1 & -\frac{\Omega_1}{2}e^{-i\omega_1 t} & 0 \\ -\frac{\Omega_1^*}{2}e^{-i\omega_1 t} & E_3 & -\frac{\Omega_2^*}{2}e^{-i\omega_2 t} \\ 0 & -\frac{\Omega_2}{2}e^{i\omega_2 t} & E_2 \end{bmatrix} \tag{2.9}$$

where $\Omega_{1,2} \equiv \wp E_{1,2}$ and $E_{1,2}$ is the amplitude of the electric field for lasers 1 and 2 respectively. Following the analysis of the two level atom, we can now multiply both sides of the Shrödinger equation by a Q matrix where

$$Q = \begin{bmatrix} e^{i\theta_1 t} & 0 & 0 \\ 0 & e^{i\theta_2 t} & 0 \\ 0 & 0 & e^{i\theta_3 t} \end{bmatrix} \tag{2.10}$$

If we let δ_1 denote the detuning of ω_1 from the $|1\rangle \rightarrow |3\rangle$ resonance, $\frac{\Delta E_1}{\hbar}$, and δ_2 denote the detuning of ω_2 from the $|2\rangle \rightarrow |3\rangle$ resonance , $\frac{\Delta E_2}{\hbar}$, then the commmon detuning δ and the relative detuning Δ can be written in terms of δ_1 and δ_2. Namely, $\delta \equiv \frac{1}{2}(\delta_1 + \delta_2)$ and $\Delta \equiv \delta_1 - \delta_2$. Figure A-2 shows how the frequencies of the lasers relate to the atom's energy levels. Choosing $\theta_1 = \frac{1}{\hbar}(E_1 - \frac{\Delta}{2})$, $\theta_2 = \frac{1}{\hbar}(E_3 + \frac{\Delta}{2})$, and $\theta_3 = \frac{1}{\hbar}(E_2 + \delta)$ and following the same procedure that was followed for the two level atom yields

$$\tilde{\tilde{\mathbf{H}}} = \frac{1}{2}\begin{bmatrix} \Delta & -\Omega_1 & 0 \\ -\Omega_1^* & -2\delta & -\Omega_2^* \\ 0 & -\Omega_2 & -\Delta \end{bmatrix} \tag{2.11}$$

This Hamiltonian governs the evolution of a 3 level atom in the presence of two

lasers with different frequencies. Let's review how we got to this point. First, a perturbation $V = -\vec{\rho} \cdot \vec{E}$ was added to the free space Hamiltonian for a three level atom. Then we made the rotating wave approximation. Finally, a unitary was performed with the Q matrix. By properly choosing θ_1, θ_2, and θ_3 in the Q matrix, H was transformed to a time independent form. For notational convenience the double tilde over the Hamiltonian will be dropped and henceforth H will be used to denote the time independent Hamiltonian in equation 2.11.

In the laboratory the intensities of the laser beams can be choosen so that $\Omega_1 = \Omega_2 = \Omega$. (Recall that $\Omega_{1,2} \equiv \wp E_{1,2}$.) Also, the frequencies of the laser beams can be adjusted so that there is no relative detuning, ie $\Delta = 0$. Under these conditions the Hamiltonian becomes

$$H = \frac{1}{2}\begin{bmatrix} 0 & -\Omega & 0 \\ -\Omega^* & -\delta & -\Omega^* \\ 0 & -\Omega & 0 \end{bmatrix} \tag{2.12}$$

Solving the Shrödinger equation with $|\psi\rangle = C_1|1\rangle + C_2|2\rangle + C_3|3\rangle$ yields equations for the coefficients

$$i\hbar\dot{C}_1 = -\frac{\Omega}{2}C_3 \tag{2.13}$$

$$i\hbar\dot{C}_2 = -\frac{\Omega}{2}C_3 \tag{2.14}$$

$$i\hbar\dot{C}_3 = -\frac{\Omega^*}{2}C_1 - \frac{\Omega^*}{2}C_2 - \delta C_3 \tag{2.15}$$

Now, assume that the common detuning of the two Raman beams is choosen so that it is much greater than the Rabi flopping frequency, $\delta \gg \Omega$. Under this assumption the approximation that $\dot{C}_3 = 0$ is valid. Using this approximation yields

$$C_3 = -\frac{\Omega^*}{2\delta}(C_1 + C_2) \tag{2.16}$$

Substituting into 2.13 and 2.14 we find that

$$\dot{C}_1 = \dot{C}_2 = -i\frac{\epsilon}{\hbar}(C_1 + C_2) \tag{2.17}$$

where $\epsilon \equiv \frac{|\Omega|^2}{4\delta}$. Solving these equations for an atom in state $|1\rangle$ at time $t = 0$, we find that

$$C_1 = e^{-i\frac{\epsilon}{\hbar}t}\cos\frac{2\epsilon}{\hbar}t \tag{2.18}$$

and

$$C_2 = ie^{-i\frac{\epsilon}{\hbar}t}\sin\frac{2\epsilon}{\hbar}t \tag{2.19}$$

The probability of finding the atom in state $|2\rangle$ oscillates sinusoidally

$$|C_2|^2 = \sin^2\frac{2\epsilon}{\hbar}t \tag{2.20}$$

This result is analgous to the two level atom that we discussed in the previous section. The atom Rabi flops between states $|1\rangle$ and $|2\rangle$ with frequency $\frac{2\epsilon}{\hbar}$ while the probability of finding the atom in state $|3\rangle$ always remains negligible.

Thus, we have theoretically derived a way to transfer atoms from one ground state to another ground state without the atom ever being in an excited state. For the experiment it is essential that the probability of finding an atom in an excited state remains negligible because when an atom is excited there is a chance of spontaneous emission and spontaneous emission eliminates the quantum coherence that we rely upon to see interference.

The Raman transition was derived by assuming that the electric field of the laser behaves classically. However, in quantum mechanics the photons that carry the electromagnetic field also carry a discrete quanta of energy $E = \hbar\omega$, momentum $p = \hbar k$, and can carry angular momentum. In order to understand the Raman pulse beam splitting technique all of these factors must be taken into account.

Because photons carry a momentum $p = \hbar k$, where $k = \frac{2\pi}{\lambda}$, an atom not only

absorbs the photon's energy when it becomes excited, it also absorbs the photon's momentum. Hence, an atom initially in the state $|1, p\rangle$ – where p is the momentum of the atom in the +z direction – will transition to the state $|3, p + \hbar k_1\rangle$ when a π pulse with frequency ω_1 is applied in the +z direction. In order to conserve both energy and momentum, a photon is removed from the electric field during this process. Similarly, an atom initially in $|3, p\rangle$ will transition to $|1, p - \hbar k_1\rangle$ while emitting a photon with frequency ω_1 in the +z direction when the same pulse is applied. Again, energy and momentum are conserved because of the photon that is added to the electromagnetic field. If the frequency of the laser is changed to ω_2 then an atom initially in the state $|3, p\rangle$ will transition to the state $|2, p + \hbar k\rangle$ when a π pulse is applied in the -z direction. During this process the atom emits a photon with frequency ω_2 in the -z direction.

What happens during a Raman transition is more complex. The situation is this: two lasers, one with frequency $\omega_1 + \delta$ in the +z direction and one with frequency $\omega_2 + \delta$ in the -z direction, are applied to an atom initially in the state $|1, p\rangle$. The first laser couples the states $|1, p\rangle$ and $|3, p + \hbar k\rangle$, while the second laser couples $|3, p + \hbar k\rangle$ to $|2, p + 2\hbar k\rangle$. (Here I have made the approximation that the wavelengths of the two lasers are equal, $k_1 = k_2 = k$, for simplicity.) As before if the two lasers are applied for a time corresponding to a π pulse, then a transition from the state $|1, p\rangle$ to $|2, p + 2\hbar k\rangle$ will occur. When the atom makes this transition it absorbs a photon propagating in the +z direction and emits a photon in the -z direction. Hence, the net effect is that the atom gains $2\hbar k$ of momentum in the +z direction.

There is still one detail that has been omitted: conservation of angular momentum. A circularly polarized photon carrys one quanta of angular momentum along its direction of propagation. The direction of the angular momentum depends on whether the photon is right hand circularly polarized or left hand circularly polarized. Likewise, the magnetic sublevels, denoted by the m_f quantum number, of an atom carry different amounts of angular momentum along the quantization axis of the atom. So, when an atom absorbs a photon the photon will cause a transition between two levels with different m_f numbers if the photon is circularly polarized and is

traveling along the quantization axis of the atom. The quantization axis of an atom is always in the direction of any magnetic field that is present. So, the quantization axis of an atom can be fixed by applying a slight magnetic field in the appropriate direction.

Notation is often confusing when dealing with the direction of angular momentum carried by a photon. For the rest of this paper σ_+ will be used to denote a beam that has positive angular momentum along its axis of propagation, not its direction of propagation. So, a σ_+ beam propagating in the +z direction has angular momentum in the +z direction. However, a σ_+ beam propagating in the -z direction also has angular momentum in the +z direction. This notation makes sense if the laser beam is viewed from the atom's perspective. To the atom the only thing that matters is the direction of the angular momentum, not whether the photon is right or left circularly polarized.

Consider applying a σ_+ polarized π pulse with frequency ω_1 in the +z direction to an atom initially in the state $|1, p, m_f = 0\rangle$, where m_f denotes the angular momentum along the atom's quantization axis. If the atom's quantization axis is along the z axis, then the atom will transition to the state $|3, p + \hbar k, m_f = +1\rangle$ since this state has one more quanta of angular momentum in the z direction than $|1, p, m_f = 0\rangle$. Otherwise angular momentum for the system would not be conserved. Similarly, an atom initially in $|3, p, m_f = +1\rangle$ will transition to $|2, p + \hbar k, m_f = 0\rangle$ when a σ_+ polarized π pulse with frequency ω_2 in the -z direction is applied. The atom has one less quanta of angular momentum after the transition because the atom will emit a σ_+ photon during the transition.

So, in order to induce a Raman transition from $|1\rangle$ to $|2\rangle$ using two σ_+ polarized beams, $|3\rangle$ must have one more quanta of angular momentum along the z axis than $|1\rangle$ and $|2\rangle$. Finally, all of the quantum mechanics has been explained and the reader is in a position to understand how the atomic beam is split.

2.3 Raman Pulse Beam Splitting

The ultimate goal of the experiment is to split an atomic beam in two dimensions in order to produce a two dimensional interference pattern. However, because the ideas behind one dimensional beam splitting are the same as those for two dimensional beam splitting, a one dimensional beam splitter will be considered first, for simplicity. The two dimensional beam splitter will be explained in the next section.

2.3.1 One Dimensional

To simplify the following discussion we will assume that the atomic beam is ideal: all of the atoms start in the same state, have the same speed, and travel in the +y direction. In reality the atoms are in a thermal distribution of states, travel with a Boltzmann distribution of speeds in the +y direction, and have a transverse velocity spread. (However, these non-idealities can be compensated for. Performing magnetic sub-level optical pumping transfers a majority of the atoms to the same state. Also, it is possible to cool the atomic beam with lasers in order to decrease the transverse velocity spread.)

Only 3 levels of the ^{85}Rb atom play a role in beam splitting: $|a\rangle \equiv |F = 3, m_f = 0, groundstate\rangle$, $|c\rangle \equiv |F = 2, m_f = 0, groundstate\rangle$, and $|d\rangle \equiv |F = 3, m_f = +1, excitedstate\rangle$. Figure A-3 shows the relevent energy levels of ^{85}Rb. We will assume that initially all of the atoms are in the state $|a, p = 0\rangle \equiv |a, 0\rangle$, where p is momentum of the atom in the +z direction.

The first step is to put the atoms into an equal superposition of $|a, 0\rangle$ and $|c, -2\hbar k\rangle$ by inducing a Raman transition via $|d, -\hbar k\rangle$. This is done by applying two counter-propagating σ_+ laser beams with appropriate frequencies along the z axis for a time that corresponds to a $\frac{\pi}{2}$ pulse. The laser in the -z direction is used to couple $|a\rangle$ to $|d\rangle$ and will be called laser A. The laser propagating in the +z direction is used to couple $|d\rangle$ to $|c\rangle$ and will be called laser C. Applying both lasers at the same time induces a Raman transition between $|a\rangle$ and $|c\rangle$.

After creating an equal superposition of $|a\rangle$ and $|e\rangle$ another pulse is applied, but

this time the directions of the A and C pulses are switched and the duration is extended to correspond to a π pulse. So, the portion of atoms in $|a,0\rangle$ transitions to $|c,+2\hbar k\rangle$, while the portion of atoms in $|c,-2\hbar k\rangle$ transitions to $|a,-4\hbar k\rangle$. Thus, after the second pulse pair the system is in an equal superposition of $|a,-4\hbar k\rangle$ and $|c,+2\hbar k\rangle$. It is important to note that two Raman transitions occur in parallel. $|a,0\rangle$ Raman transitions to $|c,+2\hbar k\rangle$ via $|d,+\hbar k\rangle$, while $|c,-2\hbar k\rangle$ is coupled to $|a,-4\hbar k\rangle$ via $|d,-3\hbar k\rangle$. Because the intermediate $|d\rangle$ state is different for both of these Raman transitions - one $|d\rangle$ state has $p=+\hbar k$ while the other has $p=-3\hbar k$ – there is no mixing of the two Raman transitions, ie they occur independently. For the third set of pulses the directions of A and C are again reversed and the duration is choosen to correspond to a π pulse. The portion of the atoms in state $|a,-4\hbar k\rangle$ transition to $|c,-6\hbar k\rangle$, while the portion of atoms in state $|c,+2\hbar k\rangle$ transition to $|a,+4\hbar k\rangle$. After this, the atoms are in an equal superposition of $|a,+4\hbar k\rangle$ and $|c,-6\hbar k\rangle$. Applying π pulse pairs continues while alternating the directions of the A and C beams. After P pulse pairs the system will be in an equal superposition of $|a,+2P\hbar k\rangle$ and $|c,-(2P+2)\hbar k\rangle$. Figure A-4 is a diagram which shows how the pulses are applied. Because the two components of the atomic beam have momentum in different directions, one has momentum in the +z direction while the other has momentum in the -z direction, the two components of the atomic beam will separate spatially.

Once the beams have become sufficiently separated, a set of 2P pulse pairs is applied in order to reverse the momentum of the two components of the atomic beam along the z axis. This is achieved using the same method that was used to split the beam, ie apply π pulse pairs while alternating the directions of the A and C pulses. For example, the first pulse pair that is applied to recombine the atomic beam has the A and C coming from the same directions that they came from during the last pulse pair of the splitting process. The effect is to cause the atoms in $|a,+2P\hbar k\rangle$ to transition to $|c,(2P-2)\hbar k\rangle$, while causing the atoms in $|c,-(2P+2)\hbar k\rangle$ to transition to $|a,-2P\hbar k\rangle$. After all 2P pulses have been applied the atoms will be in an equal superposition of $|a,-2P\hbar k\rangle$ and $|c,+(2P-2)\hbar k\rangle$. Hence, the two components of the atomic beam will be traveling towards one another. The path that the atoms will

take is like the path shown in figure A-1.

While the two components of the beam are moving towards one another, but are still spatially separated, a pair of linearly polarized laser pulses, co-propagating in the +x direction are applied only to the component of the beam corresponding to $|c, +(2P-2)\hbar k\rangle$. The duration of the pulse pair is chosen to cause a π transition from $|c\rangle$ to $|a\rangle$. Because the beams are co-propagating no momentum is transferred to the system in the x direction. Hence, the final state of the atoms is an equal superposition of $|a, -2P\hbar k\rangle$ and $|a, +(2P-2)\hbar k\rangle$.

Eventually, the two components of the atomic beam will intersect spatially. If a plate is placed at this intersection point to stop the atoms, then the wave nature of the atoms will cause interference fringes on the plate. In other words, atoms will not be plated on certain parts of the plate due to destructive interference between the wave functions of the two components of the atomic beam at that point in space. Many atoms will be plated in areas where constructive interference occurs. The net result is that the atoms on the plate will form a finely spaced grating.

This setup can also be used to detect rotations. The basic idea is that if the apparatus rotates while the atoms are in flight, then the path lengths that the atoms in different branches of the atomic beam will be different. This will cause the interference fringes to shift position.

2.3.2 Two dimensional

The scheme for splitting the atomic beam in two dimensions is a simple extension of the ideas used to spilt the atomic beam in one dimension. The two dimensional beam splitter starts in the same way that the one dimensional beam splitter starts. A series of pulses are applied to split the atomic beam along the z axis and then to recombine it. However, immediately after the 2P pulse pairs are applied to recombine the atomic beam, another series of pulses is applied to split the atomic beam along the x axis. These pulses follow exactly the same format that was used to split the atomic beam along the z axis, only this time the pulses are applied along the x axis. The net effect is that while the atoms are traveling towards one another in the z

direction, they are split and recombined in the x direction. By choosing parameters correctly the four portions of the atomic beam can be made to spatially intersect at the same point in space. By placing a plate at this point, the atoms will interfere to create a two dimensional pattern on the plate. Figure A-5 shows how this splitting might look if it were used to split atoms falling from an atom trap.

After the 2P pulses to recombine the atoimc beam along the z axis, the atoms are in an equal superposition of $|a, -2P\hbar k\rangle$ and $|c, +(2P-2)\hbar k\rangle$. A $\frac{\pi}{2}$ pulse is then applied with counter-propagating beams in the x direction. This causes the atoms to enter an equal superposition of $|a, -2P\hbar k, 0\rangle$, $|c, -2P\hbar k, -2\hbar k\rangle$, $|c, +(2P-2)\hbar k, 0\rangle$, and $|a, +(2P-2)\hbar k, -2\hbar k\rangle$, where the second momentum index refers to the atom's momentum in the +x direction.

Next a π pulse is applied with the directions of the A and C lasers switched. As a result the atoms enter an equal superposition of $|c, -2P\hbar k\rangle$, $|a, -2P\hbar k, -4\hbar k\rangle$, $|a, +(2P-2)\hbar k, +2\hbar k\rangle$, and $|c, +(2P-2)\hbar k, -4\hbar k\rangle$. This pattern of applying π pulses while alternating the direction of the A and C lasers is continued in order to split and recombine the atomic beam along the x axis.

Chapter 3

Injection Locking a Diode Laser Using a Filtered Electro-Optic Modulator Sideband

The large angle atomic interferometer requires two laser beams with a controllable difference in frequencies. This chapter reports on realizing this goal using a technique where an electro-optic modulator sideband is filtered through a cavity and injected into a diode laser, in a novel configuration yielding very high feedback isolation without sacrificing access to the output power of the diode laser. The advantages of this approach over alternative techniques for injection locking are discussed.

Many experiments in atomic physics require generation of two laser beams that have an extremely high degree of phase coherence with one another. For frequency differences on the order of a few hundred megahertz, an acousto-optic modulator (AOM) can be used to directly produce a frequency shifted beam with high efficiency. However, AOMs that can shift a laser beam by a few gigahertz (e.g. 6.8 GHz for ^{87}Rb) have efficiencies close to one percent or less, and hence do not produce a frequency shifted beam with power that is adequate for most experiments.

For example, in order to excite Raman dark resonances between the metastable hyperfine states of ^{85}Rb, one requires two laser beams with frequencies separated by 3 GHz. It is also necessary to have a significant amount of power (of the order of

few 10's of mW) in each beam. An AOM or an electro-optic modulator (EOM) can be used to produce a 3 GHz shift in frequency, but neither will produce a shifted beam with adequate power. However, one can use injection of external irradiation to lock a diode laser to the shifted beam produced by an AOM or EOM in order to increase the power of the frequency shifted beam. The general concept of injection locking involves the use of a master laser operating at low power and efficiency, but producing a stable single mode output beam which is then injected into the resonant cavity of a high-power slave laser. Injection locking was first demonstrated by Stover and Steier, who directly injected a beam from a He-Ne laser into another laser. Since that time injection locking has been studied theoretically and experimentally.

One of the drawbacks of using an AOM shifted beam is that the diffracted beam changes direction as the frequency is tuned. As a result, coupling between master and slave lasers is varied so that the frequency range available for stable locking becomes very limited. Since many experiments, including ours, require the ability to tune the difference frequency over a broad range, this beam misalignment imposes severe constraints on experimental setup, requiring additional compensation techniques. On the other hand, the sidebands produced by an EOM are always co-propagating with the fundamental frequency, so that no misalignment occurs due to frequency tuning. This gives an EOM a clear advantage over an AOM in an injection locking scheme. Furthermore, in general the frequency shift achievable using an EOM is much larger than that achievable using an AOM. Finally, the EOM approach is analogous to yet another approach where the master laser is modulated directly; such an approach will eliminate the need for any external modulator, which is important for miniaturization efforts.

However, the EOM approach (and the direct laser modulation approach) has some obvious potential difficulties. First, the desired modulation sideband needs to be filtered using a cavity with a high enough finesse so that the leakage from the intense fundamental frequency component is negligible. Second, the diode laser output may reflect back to itself from the surface of the cavity mirrors, causing instability. A simple isolation scheme often results in a configuration where only a part of the diode

laser output is accessible for use as a single beam. In this paper, we report on our successful demonstration of realizing the EOM approach for locking a diode laser to a 3 GHz shifted sideband of a Ti-Sapphire laser using a novel isolation scheme that circumvents these problems.

A schematic of the setup that we used is shown in Figure A-6. A Coherent 899 single mode tunable Ti-Sapphire ring laser is used as a master laser to produce a fundamental optical frequency. The laser operates near 780.245 nm with frequency jitter estimated to be less than 1 MHz. The laser beam is sent through an EOM (New Focus model 4431) and driven by a 3 GHz high-frequency source that is phase locked to a rubidium atomic clock. The EOM outputs a laser beam with three frequency components, the fundamental frequency and two $\pm$ 3 GHz shifted sidebands that are co-propagating. The intensity of each sideband is about 4% of the fundamental component intensity. The output beam is then sent through a home-made Fabry Perot cavity with finesse of $\sim$ 60 and a free spectral range of about 30 GHz in order to eliminate the fundamental and one of the sidebands components from the injection beam. To implement this, the cavity is first manually tuned to the transmission peak of the desired sideband, and then kept locked to this peak by standard electronics. The resulting output beam, shifted by 3 GHz from the frequency of the Ti Sapphire beam, is then sent into a diode laser after passing through a polarizing broad band cube beamsplitter and a modified Faraday isolator. Both the polarizing cube beam splitter and the modified optical isolator play a key role in our experimental setup and will be described below. Finally, the beam is fed into an SDL 5412 diode laser. Coarse longitudinal mode matching is accomplished by controlling the temperature of the laser. Fine tuning is achieved by adjusting the drive current. Transverse mode matching is produced by proper selection of collimating optics. The coupling between the injected field and the diode laser is varied for optimal locking by means of a set of neutral density filters. The most stable locking was achieved with injection power range of 1.0 - 0.5 μW. The injection locked diode laser produces a single mode beam, which is 3 GHz shifted relative to the fundamental frequency of Ti-Sapphire laser, with more than 100 mW of power.

It is well known that due to the combination of low facet reflectivities, small cavity length, and high gain, feedback has a deleterious effect on semiconductor lasers. A feedback level of -70 dB is considered very low and hardly causes any effect in the diode laser behavior. However, a level of -40 dB will have a dramatic effect on a system's performance. Optical feedback commonly originates from unwanted reflections coming from lenses and other optical elements. In our system, a strong unavoidable reflection from the cavity is considered to be the major contributor to the optical feedback. It is instructive to point out that even a perfect optical isolator would be unsuitable for our injection locking setup since it would stop all of the injection laser power. Therefore, one of the major challenges in the injection locking system is to block the reflected diode laser light and to allow external optical injection beam to penetrate into the diode laser. We solved this problem by creating a special optical system based on a modified optical isolator and a polarizing cube beamsplitter, which utilizes the initial difference in polarization of the diode laser and the external injection beam.

In order to illustrate how the modified isolator works we recall briefly how a regular isolator works and then discuss the modification we made to our isolator. A regular isolator consists of three basic pieces in series: a vertical polarizer, an optically-active material that rotates the polarization non-reciprocally by +45 degrees, and a linear polarizer oriented at +45 degrees. Figure A-7a shows a diagram of a regular isolator with a reflected beam entering from the right and a direct diode laser beam entering from the left. First, consider the direct diode laser beam. The vertically oriented polarizer eliminates the horizontal component of the incoming beam (if it is present) while allowing the vertical component to continue. The beam, now vertically polarized, is then rotated by +45 degrees. Finally, the beam passes through a polarizer oriented at +45 degrees without attenuation. The net effect is that the vertical component of the direct laser beam will pass through the isolator, but it will be rotated by +45 degrees at the output. Next, consider the reflected beam. No matter how the beam is initially polarized, after it passes through the first polarizer it encounters, it becomes polarized in the direction of the polarizer, +45 degrees. This polarization

is then rotated by +45 degrees resulting in a horizontally polarized beam. Since the vertical polarizer and the beam are cross-polarized, the beam can not penetrate into the diode laser.

Our modified isolator is just like a regular isolator only without the linear polarizer oriented at +45 degrees (see Figure A-7b). We used a standard diode laser isolator from Electro-Optics Technology, Inc. According to the manufacturer's specification, this device provided isolation of better than 30 dB. Removal of the polarizer does not affect direct laser beams passing through the isolator. However, an injection beam traveling to the left and polarized at -45 degrees can now pass through the isolator without attenuation. Of course, with its polarization being rotated by +45 degrees, it becomes vertically polarized.

To understand how all of the elements work together we have to consider the transformation of the polarization of the beams as they travel through the experimental setup. Figure A-6 shows the polarization of the injection beam, and the direct and reflected diode laser beams at different points. The Ti-Sapphire laser beam is initially circularly polarized. After passing through the EOM and the Fabry Perot cavity, the beam is shifted by 3 GHz and has only about 0.5 % of its original power (the cavity transmission is about 13%). The beam then passes through a quarter wave plate that changes the polarization from circular to vertical. After being reflected by the polarizing beam splitter, the shifted beam passes through the half-wave plate and becomes polarized at -45 degrees. The beam continues through the modified isolator to the diode laser. The direct diode laser beam is initially vertically polarized. It passes through the modified isolator with no power loss, but is rotated by +45 degrees. The half wave plate then rotates the beam by another +45 degrees so that the diode laser beam is horizontally polarized before entering the polarizing beam splitter. Thus, nearly all of the diode laser power continues through the polarizing splitter, which only reflects vertically polarized light, to the experiment. Note that the modified isolator converts counter-propagating beams with parallel polarizations to cross polarized beams. Without the modification, the polarizations of the diode laser beam and the injection beam would always match at the diode laser (as they

must in order for injection locking to work) and hence the beam splitter would not separate the diode laser beam path from the Ti-Sapphire beam path.

The quarter wave plate is oriented so that the residual fraction of the direct diode laser beam that is reflected by the polarizing beam splitter becomes circularly polarized after passing through it. The reflected beam passes through the quarter wave plate a second time and is converted from circularly polarized to horizontally polarized. Again, the major part of reflected beam passes straight through the polarizing beam splitter and is prevented from feeding back to the diode laser. In other words, our setup effectively filters the cavity-reflected diode laser beam twice. When the main diode laser beam is sent through the polarizing beam splitter only a small fraction of the beam ($\delta \approx 3\%$) is reflected. Part of the reflected beam then reflects off of the cavity and returns to the polarizing beam splitter. Again only a small fraction (δ) of this light is reflected back towards the diode laser. In the end a maximum of (δ^2 of the diode laser beam feeds back to the diode laser. As a result, this configuration provides feedback attenuation on the level of 30 dB. A set of neutral density filters (NDF) used to vary intensity of the injected beam is providing an additional feedback isolation up to 20 dB (for an NDF setting of 10 dB) without affecting the useful output intensity of the diode laser. When the NDF is set at a lower value, the feedback suppression is reduce, while the intensity of the injection beam is increased. We observed that under this condition (NDF less than 10 dB), the diode lasers became multimode if the injection beam was blocked, because of the residual feedback. However, when the injection beam was unblocked, the laser became single-mode, and locked to the desired EOM sideband. For NDF less than 5 dB, the feedback could no longer be overcome by the injection beam.

In order to test the degree to which the diode laser was phase-locked to the sideband of the Ti-Sapphire laser, we sampled a part of the injection beam, and shifted it with a 270 MHz AOM. This beam was then combined with a sample from the diode laser output, and the beat note was detected using an APD detector. Figure A-8 shows that the width of this beat note is about 2 kHz, which is essentially the resolution limit of the spectrum analyzer used. Fundamentally, we expect the beat-

note to be much narrower, limited only by the noise in the servo used to phase lock the 3 GHz high-frequency source to the rubidium clock.

To determine the degree of phase-locking more precisely, we also used this injection locking scheme to observe Raman-Ramsey fringes. The 1.2 kHz width of the fringes, shown in Figure A-9, is very close to the transit time limited value. The damping rate of the fringes, caused by the longitudinal velocity spread, is in agreement with the theoretical velocity distribution. The zone separation is 30 cm, and the mean atomic velocity is $\sim 300m/sec$, so that the expected transit time width is about 1 kHz. The observed linewidth here is about 1.2 kHz, where the additional width is attributable to the velocity averaging. Thus, we can conclude that the relative frequency noise between the diode laser and the Ti-Sapphire laser is less than 100 Hz. If this experiment were to be performed using trapped atoms, which would yield a much narrower ($\sim$ 1 Hz) transit-time limited linewidth, one could determine the beat-note with even better precision.

In summary, we demonstrated injection locking of a diode laser to a cavity-filtered electro-optic modulator sideband in a novel configuration yielding very high feedback isolation without sacrificing access to the output power of the diode laser. The next chapter explains how we used this technique to perform preliminary experiments.

Chapter 4

Experimental Results

Although a large angle atomic interferometer has not yet been produced, progress has been made towards achieving that goal. Experiments have been performed to characterize our system, so that proper parameters may be choosen for future experiments. This chapter discusses the experimental results that are available thus far.

4.1 Basics of the Atomic Beam

In order to understand the experimental results, one must first understand the basic experimental setup. The first step in creating the atomic beam is to place a solid sample of Rb in an oven. Heating the oven causes some of the solid to be converted to vapor. Some of the atoms in the vapor are allowed to escape from the oven via a small hole. However, the atoms which escape from the oven's hole travel in many different directions. In order to collimate the atoms into a beam, an aperture is placed along the axis of the atomic beam. For our system the two holes are 1 mm in diameter and separated by 30 cm. Figure A-10 shows a schematic of an atomic beam. Because the mean free path of the atoms in the vapor is so large, atoms travel in straight lines, rarely colliding with one another. Hence, atoms that manage to pass through both holes travel are collimated and thus form an atomic beam. However, because the apertures that define the atomic beam have a finite size, the atoms do not all travel in exactly the same direction, ie there is a transverse velocity spread to the atomic

beam.

In order to detect the presence of the atomic beam a laser beam which is resonant with an atomic transition is directed through the atomic beam. The result is that atoms are excited to a higher energy state. The excited atoms then spontaneously emit, ie decay to a ground state while emitting a photon. A photo-multiplier tube (PMT) placed above the atomic beam is used to detect the light emitted from the spontaneous decay of excited atoms. Figure A-10 shows a schematic of the detection scheme described. For the rest of this paper the laser beam that is below the PMT and is used to excite atoms is called the detection beam. We will assume that the detection beam is tuned to the $|3\rangle \rightarrow |4\rangle$ transition.

4.2 Single Zone Co-Propagating Raman

The internal states of the atoms in the atomic beam are thermally distributed when the atoms leave the oven. In our experimental setup this means that the atoms are fairly equally distributed between the $F = 2$ and $F = 3$ ground states. Moreover, the populations of the magnetic sublevels of the ground states are also fairly evenly populated.

Before a Raman transition can be detected the atoms must be optically pumped to one ground state. For example, suppose a laser beam resonant with the $|F = 3\rangle$ to $|F' = 3\rangle$ transition is applied. (For notational convenience a prime has been used to indicate an excited state. So, $|F = 3\rangle \equiv |F = 3, groundstate\rangle$ and $|F' = 3\rangle \equiv |F = 3, excitedstate\rangle$.) Atoms in $|F = 3\rangle$ will become excited, while atoms in $|F = 2\rangle$ will not be affected. The excited atoms will then decay via spontaneous emission to either ground state. Atoms that fall to the $|F = 2\rangle$ will remain there. However, atoms that fall back to the $|F = 3\rangle$ will be excited again by the laser beam to an excited state, and will decay again. This process will continue until virtually all of the atoms will enter $|F = 2\rangle$, provided that the laser beam is applied for a long enough time. This process is called optical pumping.

After optically pumping the atoms in the atomic beam to $|F = 2\rangle$, two co-

propagating laser beams are directed through the atomic beam. The frequency of one laser beam is fixed at some arbitrary detuning, while the frequency of the other laser beam can be scanned used the method described in Chapter 3. When there is a large relative detuning Δ between the two lasers, no Raman transition takes place in the atoms. However, when the relative detuning is zero some of the atoms will be transferred to $|F = 3\rangle$ via a Raman transition.

Now consider scanning the frequency of one of the lasers. When the relative detuning Δ is large, no atoms will be transferred to $|F = 3\rangle$. Hence, the PMT will not detect any fluorescence since only atoms in $|F = 3\rangle$ are detected when using the detection scheme described in section 4.1. As the detuning is decreased some of the atoms will start to be transferred to $|F = 3\rangle$ and the PMT will detect fluorescence. When the detuning is zero, the maximum number of atoms will be transferred to $|F = 3\rangle$ and thus the signal will be greatest. As the frequency of the diode laser is further increased the detuning increases and the number of atoms transferred to $|F = 3\rangle$ decreases. Figure A-11 shows experimental data for a single zone Raman transition. The peak in fluorescence occurs when $\Delta = 0$.

When a magnetic field is applied to an atom the degeneracy of the magnetic sub-levels is broken and the energies split. Figure A-3 is a detailed picture of the magnetic sub-levels of ^{85}Rb. In our experimental setup there are long Helmholtz coils that run along the length of the atomic beam. Sending current through the coils generates a magnetic field, perpendicular to the direction of the atomic beam and breaks the degeneracy of the magnetic sublevels.

Because the magnetic sublevels have different energies when a magnetic field is applied the detunings of the lasers are different for different magnetic sub-levels. For example, if a laser is resonsant with the $|F = 2, m_f = 0\rangle \rightarrow |F' = 2, m_f = 0\rangle$ transition, then it will have a non-zero detuning for the $|F = 2, m_f = +1\rangle \rightarrow |F' = 2, m_f = 0\rangle$ transition. Hence, the relative detuning Δ of the two laser beams is different for different magnetic sub-levels. Since the atoms are roughly equally distributed among the magnetic sublevels, we expect to see five Raman dips if we scan the relative detuning of the two lasers over a broad enough range. Figure A-12

shows experimental data for a co-propagating Raman experiment with a magnetic field on. As expected, the heights of the peaks are roughly equal.

4.3 Magnetic Sub-level Optical Pumping

This section describes a method for optically pumping atoms into the same magnetic sub-level. This is useful because only atoms in the $|F = 2, m_f = 0\rangle$ state contribute to the interference signal. In the large angle atomic interferometer, therefore, it is desirable to have as many atoms as possible in the $|F = 2, m_f = 0\rangle$ state. There is a simple way to achieve magnetic sub-level optical pumping using two lasers, which relies on the fact that the $|F = 2, m_f = 0\rangle \rightarrow |F' = 2, m_f = 0\rangle$ transition is forbidden due to selection rules.

Two co-propagating lasers are applied along the x axis so that they are perpendicular to both the atomic beam and the magnetic field. One laser is tuned to the $|F = 3\rangle \rightarrow |F' = 3\rangle$ transition. The purpose of this laser is to pump all of the atoms in $|F = 3\rangle$ to $|F = 2\rangle$. It is important to look carefully at what happens to the atoms when this laser is applied by itself.

Take for instance an atom in $|F = 3, m_f = +1\rangle$. When the pump laser is applied the atom is excited to $|F' = 3\rangle$. However, if the polarization of the pump beam is arbitrary then it is possible for the angular momentum of the atom to change during the transition, ie $\Delta m_f = -1, 0, or + 1$. So, the atom in $|F = 3, m_f = +1\rangle$ can be excited to $|F = 3, m_f = 0\rangle$, $|F = 3, m_f = +1\rangle$, or $|F = 3, m_f = +2\rangle$. This atom can then spontaneously decay to either $|F = 2\rangle$ or $|F = 3\rangle$. Moreover, the angular momentum along the quantization axis may change again when the atom decays, ie $\Delta m_f = -1, 0, or + 1$. So, an atom in $|F' = 3, m_f = +1\rangle$ might decay to many levels including $|F = 2, m_f = 0\rangle$.

The other laser is tuned to the $|F = 2\rangle \rightarrow |F' = 2\rangle$ transition. The polarization of this laser is choosen so that no angular momentum can be transferred to the atoms, $\Delta m_f = 0$. In other words, an atom in $|F = 2, m_f = +1\rangle$ will be excited to $|F' = 2, m_f = +1\rangle$ by this laser. However, because the $|F = 2, m_f = 0\rangle \rightarrow |F' =$

$2, m_f = 0\rangle$ transition is forbidden, once an atom enters $|F = 2, m_f = 0\rangle$ it remains there. Atoms in other magnetic sub-levels of $|F = 2\rangle$ are pumped to $|F' = 2\rangle$. Some of these atoms decay to $|F = 2, m_f = 0\rangle$ where they remain. Other atoms decay to different magnetic sublevels of $|F = 2\rangle$ and are again excited by the laser tuned to the $|F = 2\rangle \rightarrow |F' = 2\rangle$ transition. The rest of the atoms decay to $|F = 3\rangle$ where they are pumped back to $|F = 2\rangle$ by the pump laser. If the two lasers are applied for a long enough time, then all of the atoms will eventually move to $|F = 2, m_f = 0\rangle$.

Magnetic sub-level optical pumping has been performed with our experimental setup. Figure A-13 shows the experimental data. It is clear that nearly all of the atoms are pumped to the $|F = 2, m_f = 0\rangle$ sublevel.

4.4 Ramsey Fringes

The interference involved in the Ramsey fringe experiment is analgous to the interference that is seen in a double slit experiment. There are a few ways to understand how the interference arises. This section will attempt to explain the interference in the most intuitive way.

First it is necessary to learn to look at things from a different perspective. Consider taking the Fourier transform of the intensity of an arbitrary pulse of light. The key point is this: the magnitude of the Fourier transform at the atom's resonant frequency is what determines whether an atom becomes excited. For example, a pulse of radiation that is resonant with an atom has a large frequency component at the atom's resonant frequency, so an atom can become excited. However, if one were to apply a pulse of radiation that was shaped so that it had no frequency component at the atom's resonant frequency, then the atom would not become excited.

A more concrete example will clarify this point. In the Ramsey fringe experiment, two sets of co-propagating Raman pulses are applied to the atomic beam at different points. (It is important that the Raman beams come from the same lasers because this ensures that the phase difference of the laser beams where they intersect the atomic beam is fixed. Otherwise interference would be seen.) So, as an atom travels

the length of the atomic beam it first encounters an optical pumping beam which brings it to the state $|F = 2\rangle$. The atom then passes through 2 sets of Raman beams before it reaches the detection beam. Looking at the experiment from the atom's frame of reference, two Raman pulses separated in time by a time τ, where τ = distance between Raman beams/velocity of atom. The intensity and size of the Raman beams are chossen so that they correpsond to $\frac{\pi}{2}$ pulses. (See figure A-14)

To simplify matters it is convenient to pretend that the experiment is performed with a two level atom that is interacting with a single laser beam. In relaity the two levels correspond to the two ground states of a 3 level atom. The intensity of the applied laser beams can be viewed as the convolution of two delta functions separated by τ with a single pulse of width T. The Fourier transform of two delta functions is a cosine function with frequency $\omega = \frac{2\pi}{\tau}$, while the Fourier transform of the single pulse has a width $\frac{1}{T}$. Convolution in the time domain corresponds to multiplication in the frequency domain, so the Fourier transform of the set of two pulses looks like a cosine multiplied by an envelope. If the Fourier transform of the two pulses is zero and the atom's frequency, then the atom will not become excited. Likewise, the larger the Fourier transform at the atom's resonant frequency, the greater the probability of finding the atom in its excited state will be.

By scanning the frequency of the laser, the phase of the second laser will change with respect to the first. We will let l denote the path length of the laser to the first interaction zone minus the path length of the laser to the second interaction zone and ϕ denote the difference of the phases of the laser at the two interaction zones. In this case, if the frequency of the laser is changed by $\Delta\omega$ then the difference in the phases of the two lasers at the interaction zones will change, $\Delta\phi = \frac{l}{c}\Delta\omega$. In the end, one expects to see interference fringes with a frequency $\omega = \frac{2\pi}{T}$ in the detection signal.

This experiment was performed with beams separated by 30 cm. Since the velocity of the atoms in our atomic beam is $\sim 300m/s$, we find that $\tau \approx 1ms$. So, we expect to see $\sim 1kHz$ interference fringes. Figure A-9 shows the experimental results. The data agrees with theory to within the uncertainty of our calculation. Because the velocities of the atoms in the atomic beam follow a Maxwell distribution, τ is different

for different atoms and hence the frequency of the interference fringes are different for different atoms. The result is that the interference fringes get washed out after a few oscillations.

Chapter 5

Conclusion

This thesis has described the theory behind a large angle atomic interferometer and has discussed the progress that has been made on the experiment. Even though we have been successful up to this point, there is still a significant amount of work that needs to be done. Currently, we are trying to perform the simpliest posible beam splitting experiment in which only one π pulse is used to split the atomic beam. Currently it is not clear if mechanical vibrations in the current experimental setup are too great to be able to successfully split and recombine the atomic beam. If vibrations are too great then the experimetnal setup will need to be moved to a more stable environment or some clever scheme will need to be devoloped to cancel the effects of the vibrations.

If the large angle atomic interferometer is successful then it will be useful in a wide range of areas. An immediate application would be to use the ability of the interferometer to detect extremely small rotations, to test general relativity by looking for the Lens-Thirling rotation caused by frame dragging. Also, there is currently a proposal to build a quantum computer using a regularly spaced array of quantum dots. The two dimensional interferometer would provide a way to create a rectangular array of quantum dots that could be used to implement a quantum computer. Many years from now, the ideas behind the atomic interferometer described in this thesis could be extended so that the placement of individual atoms on a substrate could be controlled. This would open the door to creating nano electromechanical devices.

Appendix A

Figures

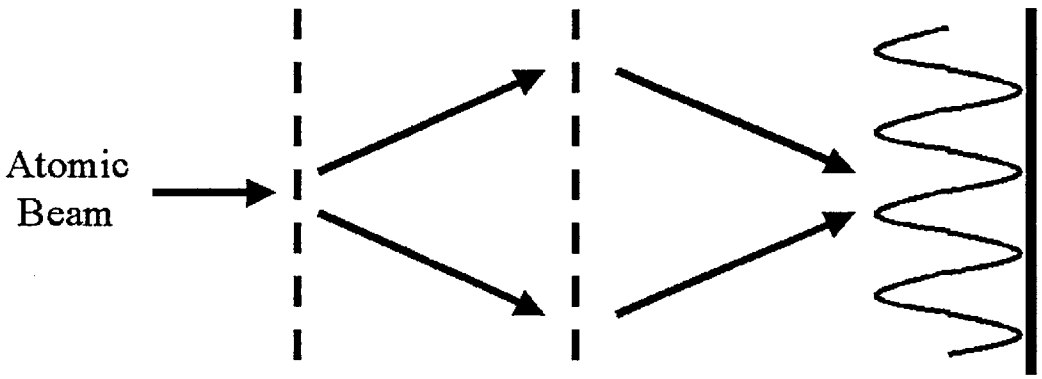

Figure A-1: Shows the basic idea behind the interference experiment. The splitting and recombining of the atomic beam, represented here by dashed lines, is achieved using a series of Raman pulses. The diagram shows that the depostion of atoms on the plate forms an interference pattern.

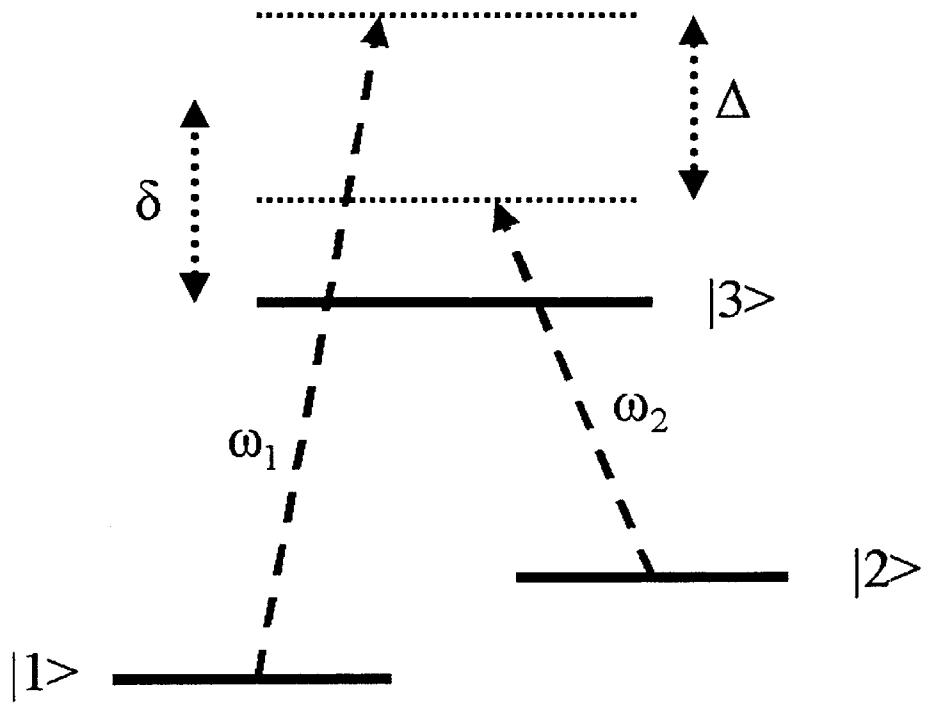

Figure A-2: Two laser beams with frequencies, ω_1 and ω_2 are applied to a three level atom to cause a Raman transition. δ is the common detuning of the laser beams. Δ is the relative detuning of the laser beams

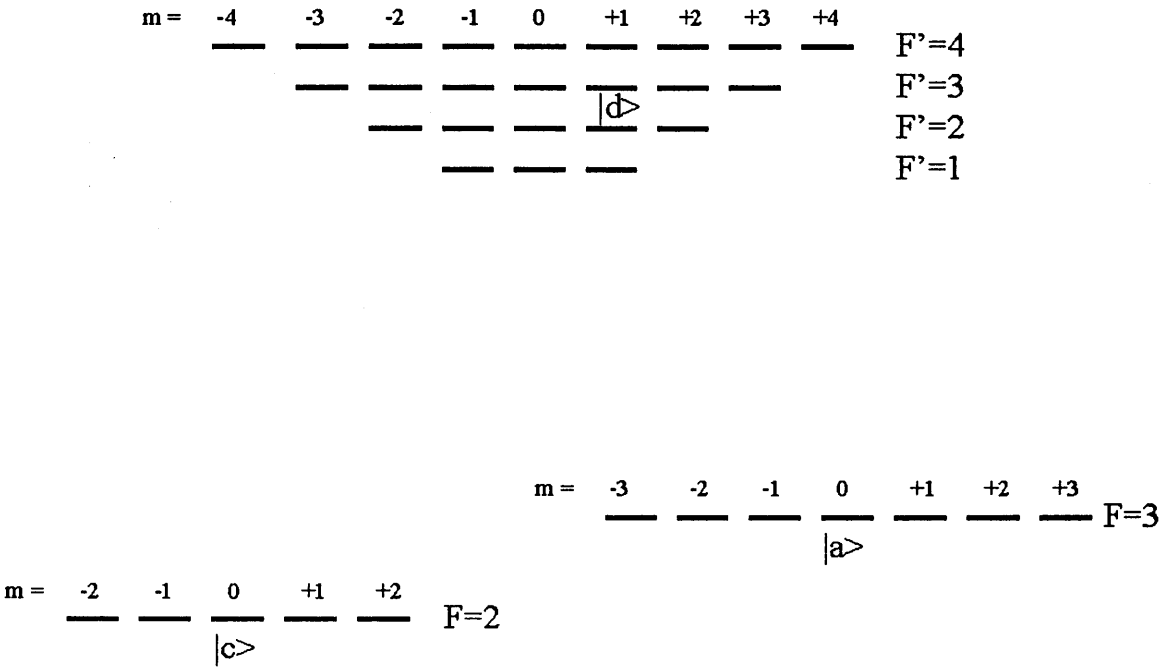

Figure A-3: Shows the relevent energy levels of ^{85}Rb.

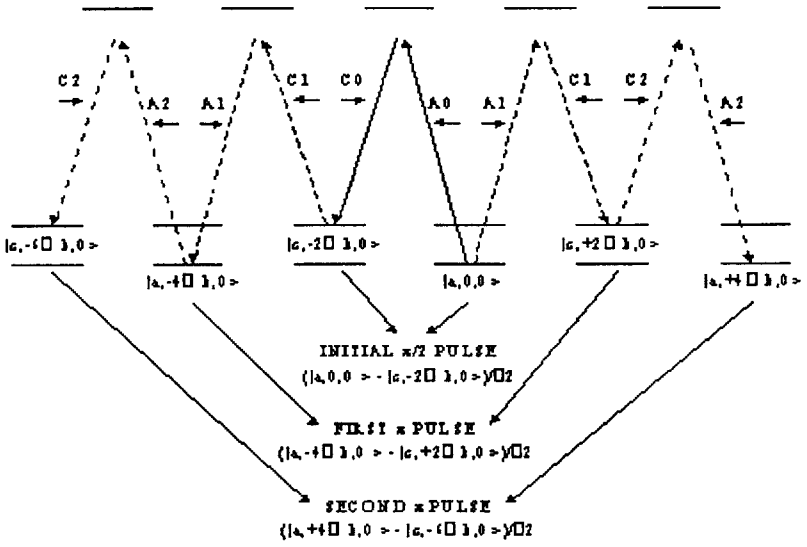

Figure A-4: Shows the first three Raman pulses used to split the atomic beam and the state of the atoms after each pulse. The first pulse, A0 and C0, is a $\frac{\pi}{2}$ pulse and puts the atoms in an equal superposition of $|a\rangle$ and $|c\rangle$. The next two π pulses give the two components of the atomic momentum in opposite directions.

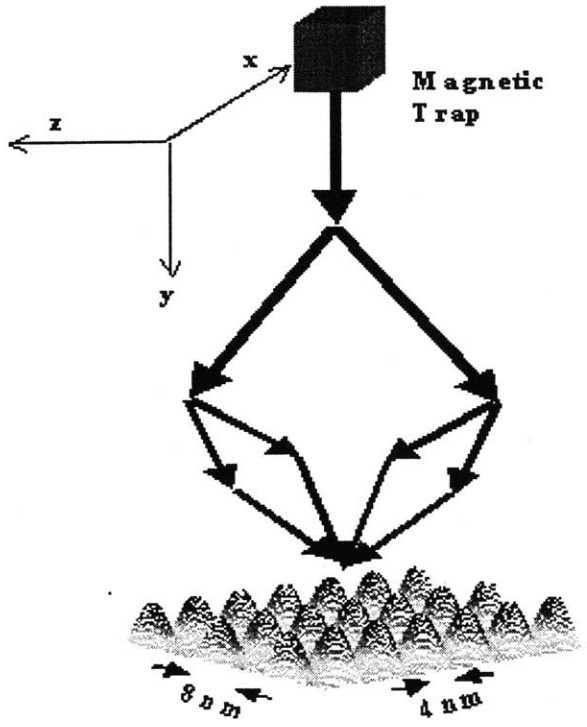

Figure A-5: Shows two dimensional Raman pulse beamsplitting applied to atoms falling from a magnetic trap. First the atoms are split along the z axis. Immediately after Raman pulses are applied to recombine the atoms in the z direction, the atoms are split along the x axis. After applying another set of Raman pulses to recombine the atoms in the x direction, all four components of the atomic beam come together to form a two dimensional interference pattern. The dimensions of the interference pattern are determined by the number of Raman pulses used to split and recombine the atoms.

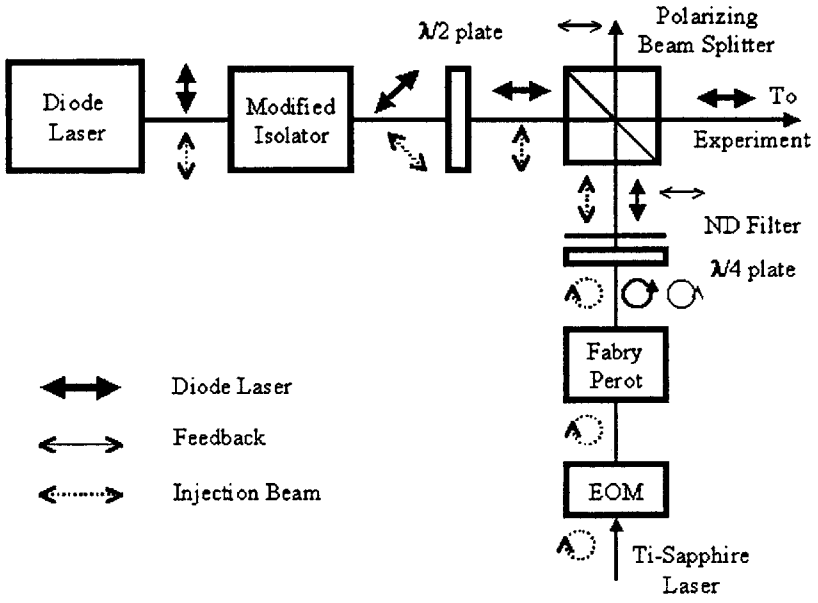

Figure A-6: Shows a schematic of the setup used to lock a diode laser to the sideband of a cavity filtered EOM shifted beam. A modified isolator is used to convert cross polarized beams to beams with the same polarization. The Fabry Perot cavity only allows the portion of the Ti-Sapphire beam that is upshifted by the EOM to pass through it. The combination of the polarizing beam splitter, neutral density filter, and $\frac{\lambda}{4}$ plate are used to minimize the diode laser power that is reflected off of the cavity and back to the diode laser.

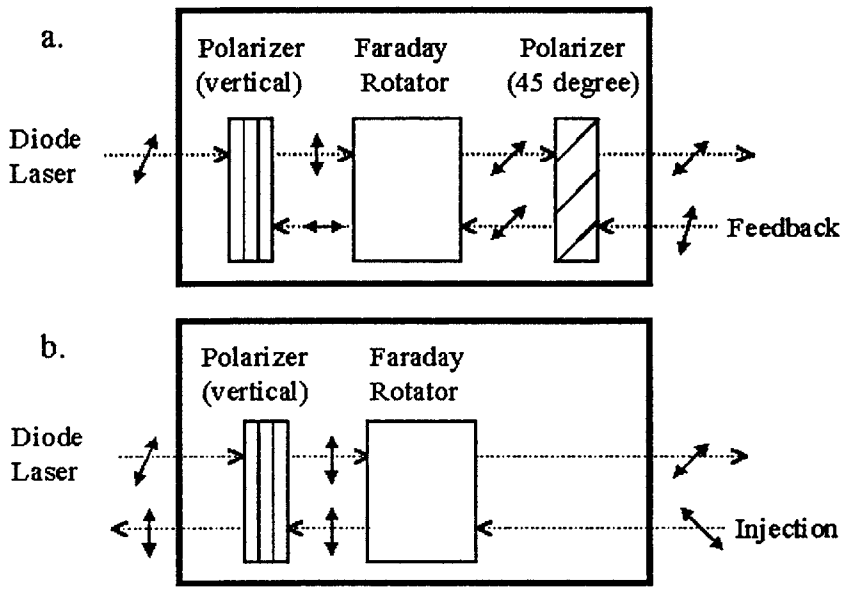

Figure A-7: a) Shows a how a normal isolator works. The combination of two polarizers with a Faraday rotator between them ensures that power can only pass through the isolator in one direction. b) Shows how we modified an isolator by removing the polarizer oriented at 45 degrees. The result is that beams that are corss polarized on the right hand side can be polarized in the same direction on the left hand side.

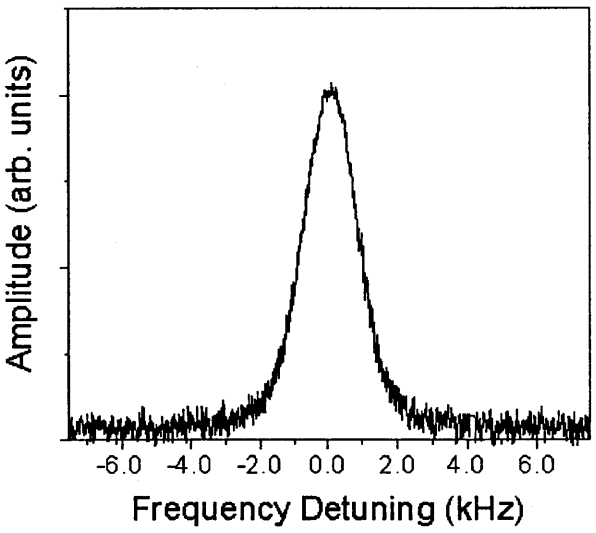

Figure A-8: Shows a beatnote generated by mixing the injection locked diode laser with a beam from the Ti-Sapphire laser.

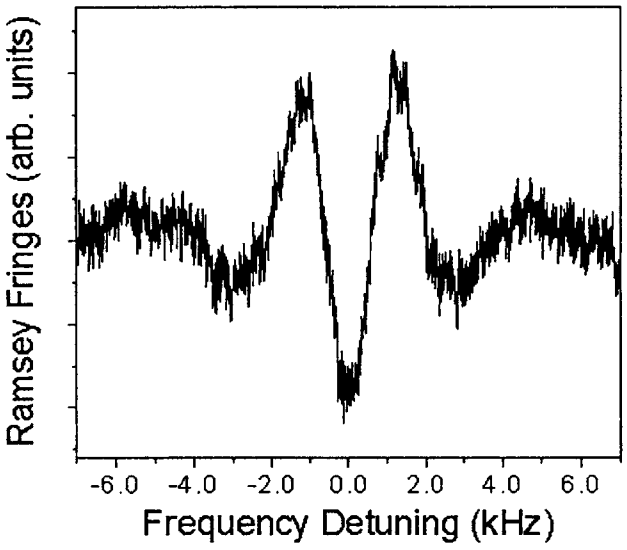

Figure A-9: The transit-time limited Raman-Ramsey fringes obtained for the magnetic field insensitive component of the off-resonant Raman transition in ^{85}Rb atomic beam.

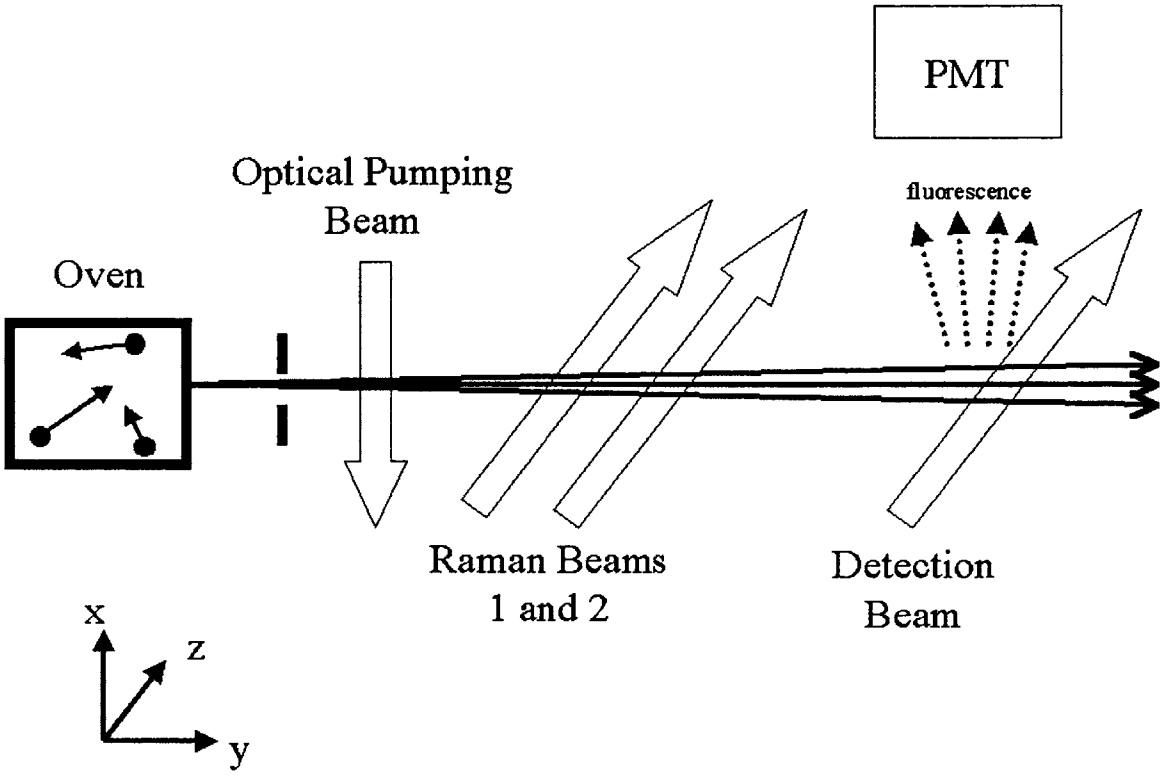

Figure A-10: Schematic of Experimental Setup. A solid sample of Rb is heated in an oven to form Rb vapor. Some Rb atoms escape from the oven through a hole and are collimated by an aperture to form the atomic beam. Optical pumping and Raman beams can be appied to the atoms as they travel the length of the atomic beam. A detection beam excites atoms in $|3\rangle$. A photo multiplier tube is used to detect photons emitted by excited atoms during spontaneous emission.

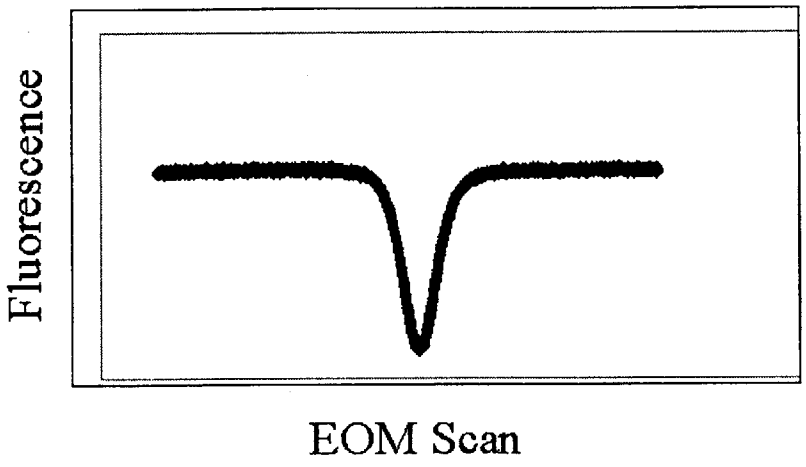

Figure A-11: Plots fluorescence detected by the PMT when one Raman beam is applied as a function of the EOM frequency shift. The peak occurs when the relative detuning of the two Raman beams is zero. (Note: fluorescence is highest at the bottom of the graph and lowest at the top of the graph.)

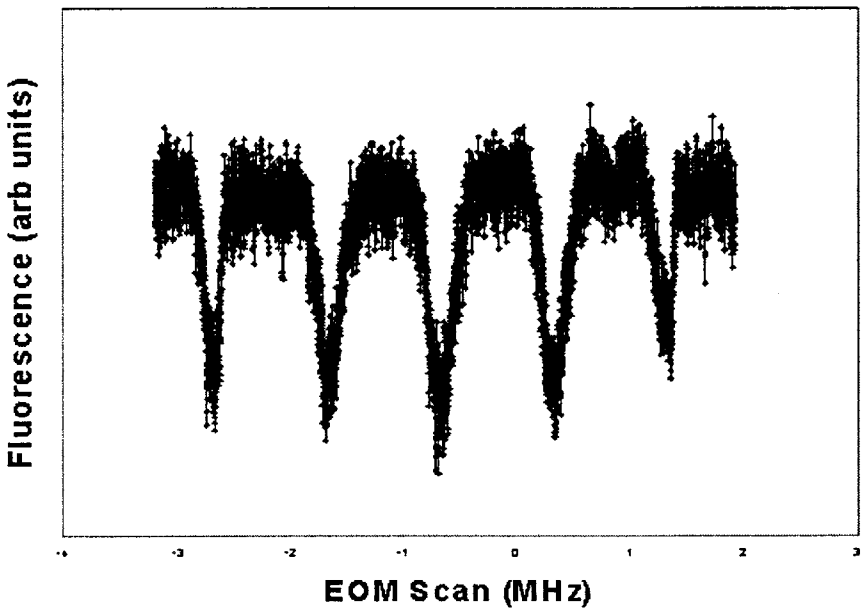

Figure A-12: Shows fluorescence plotted versus EOM frequency shift for a set of co-propagating Raman beams when a magnetic field is applied. The magnetic field splits the energies of the magnetic sublevels of $|F = 2\rangle$. The populations of the 5 magnetic sublevels of $|2\rangle$ are about equal.

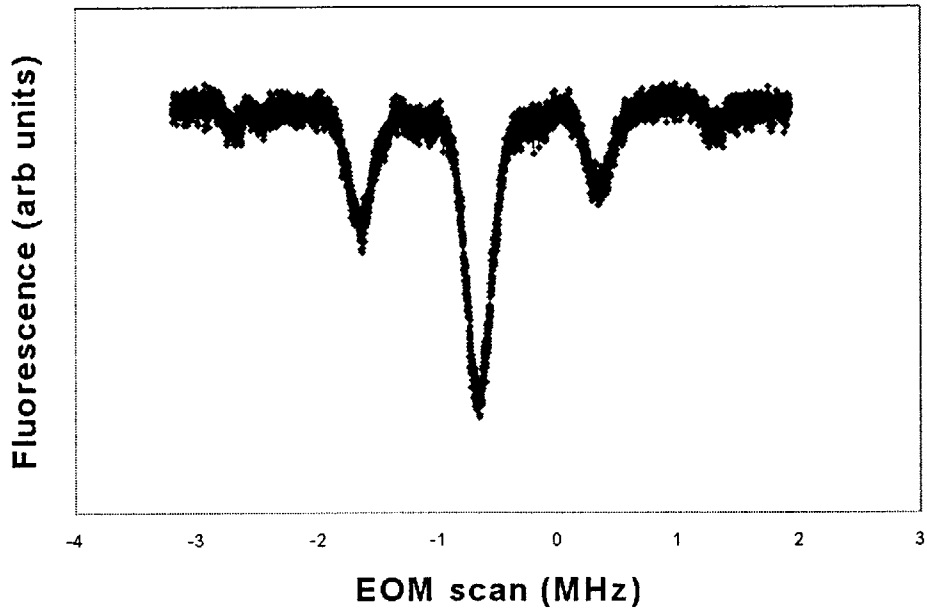

Figure A-13: Shows the effects of magnetic sublevel optical pumping. The majority of the atoms have been moved to the $m_f = 0$ state.

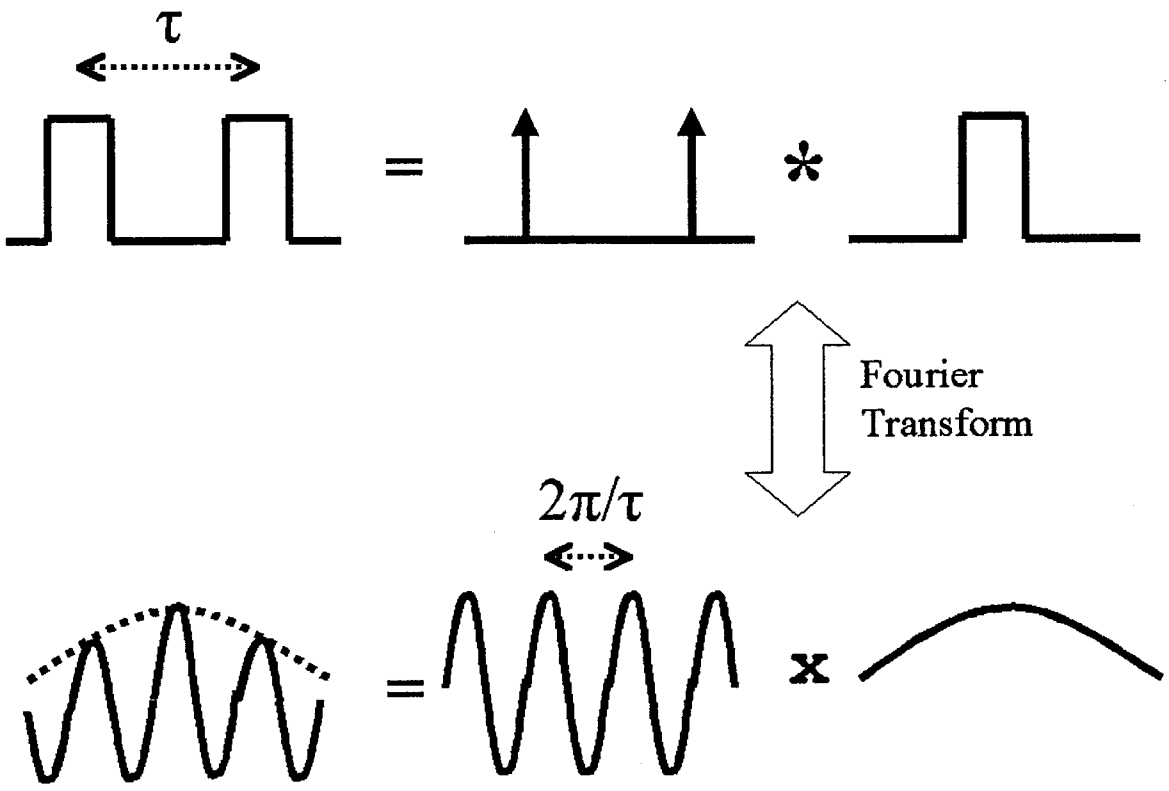

Figure A-14: Shows the two Raman pulses used to see Ramsey fringes and their Fourier transform. The top of the diagram shows the two Raman pulses separated by time τ rewritten in terms of a convolution of two delta functions with a single pulse. The bottom shows how the Fourier transform of the two pulses can be found by multiplying the Fourier transform of the two delta functions with the Fourier transform of a single pulse.

Bibliography

[1] M.R. Andrews et al., Science **275**, 637 (1997).

[2] W. Demtroder *Laser Spectroscopy* (Springer, 1998).

[3] P.L. Gould, G.A. Ruff, and D.E. Pritchard, Phys. Rev. Lett. **56**, 827 (1986).

[4] R. Grimm, J. Soding, and Y.B. Ovchinnikov, Opt. Lett. **19**, 658 (1994).

[5] T.L. Gustavson et al., Phys. Rev. Lett. **78**, 2046 (1997).

[6] P.R. Hemmer, M.S. Shahriar, M.G. Prentiss, D.P. Katz, K. Berggren, J. Mervis, and N.P. Bigelow, Phys. Rev. Lett. **68**, 3148 (1992).

[7] C.H. Henry and R.F. Kazarinov, J. Quantum Electronics, **QE-22**, 294 (1986).

[8] D. Hsiung et al., Opt. Commun., **154**, 79 (1998).

[9] U. Janicke and M. Wilkens, Phys. Rev. A. **50**, 3265 (1994).

[10] K.S. Johnson, A. Chu, T.W. Lynn, K.K. Berggren, M.S. Shahriar, and M. Prentiss, Opt. Letts. **20**, 1310 (1995).

[11] M. Kasevich and S. Chu, Phys. Rev. Lett. **67**, 181 (1991).

[12] D. Keith, C. Ekstrom, Q. Turchette, and D.E. Pritchard, Phys. Rev. Lett. **66**, 2693 (1991).

[13] W. Lawrence and D.M. Kane, Opt. Comm. **167**, 273 (1999).

[14] P. Marte, P. Zoller, and J.L. Hall, Phys. Rev. A. **44**, R4118 (1991).

[15] P. Meystre and M. Sargent III *Elements of Quantum Optics* (Springer-Verlag 1991).

[16] T. Pfau, C.S. Adams, and J. Mlynek, Europhys. Lett. **21**, 439 (1993).

[17] T. Pfau et al., Phys. Rev. Lett. **71**, 3427 (1993).

[18] M.S. Shahriar, T. Zelevinsky, and P.R. Hemmer, http://xxx.lanl.gov/abs/quant-ph/0007097

[19] M.S. Shahriar, A.V. Turukhin, T. Liptay, Y. Tan, and P. Hemmer "Demonstration of Injection Locking a Diode Laser Using a Filtered Electro-Optic Sideband" publication pending in Optics Communications (2000).

[20] M.J. Snadden et al., Phys. Rev. Lett. **81**, 971 (1998).

[21] H.L. Stover and W.H. Steier, Appl. Phys. Lett. **8**, p. 91 (1996).

[22] J.E. Thomas et al., Phys. Rev. Lett. **48**, 867 (1982).

[23] G.H.M. van Tartwijk and D. Lenstra, Quantum Semiclass. Opt. **7**, 87 (1995).

[24] C.E. Wieman and L. Hollberg, Rev. Sci. Instrum. **62**, 1 (1991).

[25] D.S. Weiss, B.C. Young, and S. Chu, Phys. Rev. Lett. **70**, 2706 (1993).

[26] M. Weitz, B.C. Young, and S. Chu, Phys. Rev. Lett. **73**, 2563 (1994).

[27] R.Younkin et al., Appl. Phys. Lett. **71**, 1261 (1997).